01 Jan 1973

Breakdown Of The Laminar Flow Regime In Permeable-walled Ducts

E. M. Sparrow

G. S. Beavers

T. S. Chen
Missouri University of Science and Technology, tschen@mst.edu

J. R. Lloyd

Recommended Citation

E. M. Sparrow et al., "Breakdown Of The Laminar Flow Regime In Permeable-walled Ducts," *Journal of Applied Mechanics, Transactions ASME*, vol. 40, no. 2, pp. 337 - 342, American Society of Mechanical Engineers, Jan 1973.
The definitive version is available at https://doi.org/10.1115/1.3422984

E. M. SPARROW

G. S. BEAVERS

School of Mechanical and Aerospace Engineering, University of Minnesota, Minneapolis, Minn.

T. S. CHEN

Department of Mechanical Engineering, University of Missouri at Rolla, Rolla, Mo.

J. R. LLOYD

Department of Mechanical Engineering, University of Notre Dame, Notre Dame, Ind.

Breakdown of the Laminar Flow Regime in Permeable-Walled Ducts

The stability of laminar flow in a parallel-plate channel having one permeable bounding wall is investigated by means of linear theory. The analysis takes account of the coupling of the disturbance fields in the channel and in the permeable material and of velocity slip at the surface of the permeable wall. Complementary experiments are performed in which the breakdown of the laminar regime in flat rectangular ducts is identified from pressure-drop measurements and from flow visualization studies. The experiments cover the range of slip velocities from 15--30 percent of the mean velocity and, in addition, the case of zero slip (impermeable walls). In the slip range of the experiments, the instability Reynolds number results of both analysis and experiment lie below the corresponding values for the case of the impermeable-walled duct. Furthermore, in this range, the instability Reynolds numbers are rather insensitive to variations in the slip velocity. Quantitative agreement between analysis and experiment was found to be somewhat better in the slip range than for the impermeable-walled duct.

Introduction

This paper is concerned, in part, with the linear stability of laminar flow in a parallel-plate channel, one of whose bounding walls is a permeable material. The laminar main flow for the stability problem consists of parallel, unidirectional flows in the channel and in the permeable material, these flows being driven by a common axial pressure gradient. The linear stability problem contains a number of novel features. First, there is coupling between the disturbance velocity and pressure fields in the channel and in the permeable wall, such that the transverse disturbance velocity need not be zero at the surface of the permeable wall. Also, there is a streamwise slip velocity at the permeable bounding surface. The existence of the slip velocity is connected with the presence of a very thin layer of streamwise moving fluid just beneath the surface of the permeable material. The fluid in this layer is pulled along by the flow in the channel. The velocity slip not only causes a skewing of the mainflow velocity profile in the channel, but also permits a nonzero streamwise disturbance velocity at the wall.

Complementary experiments were performed to investigate the breakdown of the laminar regime in flat rectangular ducts which closely approximate a parallel-plate channel. One of the two principal bounding walls of each duct was of a permeable material, whereas the other walls were solid. Identical axial pressure gradients were imposed on the flows in the channel and in the permeable wall. The breakdown of the laminar regime was deduced from the behavior of the friction coefficient and from flow visualization involving an injected dye stream.

The effect of a permeable bounding wall on laminar flow in flat rectangular ducts has been reported in earlier papers [1, 2].[1] An analytical model which contains a slip velocity at the surface of the permeable wall led to mass flow predictions which agreed well with experiment. Subsequently, Saffman [3] provided a theoretical basis for the slip velocity model. Taylor [4] and Richardson [5], in companion papers, experimentally and analytically investigated a Couette-type flow bounded by a model permeable material; excellent agreement was found to prevail between the results from the slip model and those of experiment.

The linear stability analysis comprises the main portion of the present research and will be described first. The experimental results will be presented later in the paper.

Contributed by the Applied Mechanics Division for publication (without presentation) in the JOURNAL OF APPLIED MECHANICS.

Discussion on this paper should be addressed to the Editorial Department, ASME, United Engineering Center, 345 East 47th Street, New York, N. Y. 10017, and will be accepted until July 20, 1973. Discussion received after this date will be returned. Manuscript received by ASME Applied Mechanics Division, March 6, 1972. Paper No. 72-APM-PPP.

[1] Numbers in brackets designate References at end of paper.

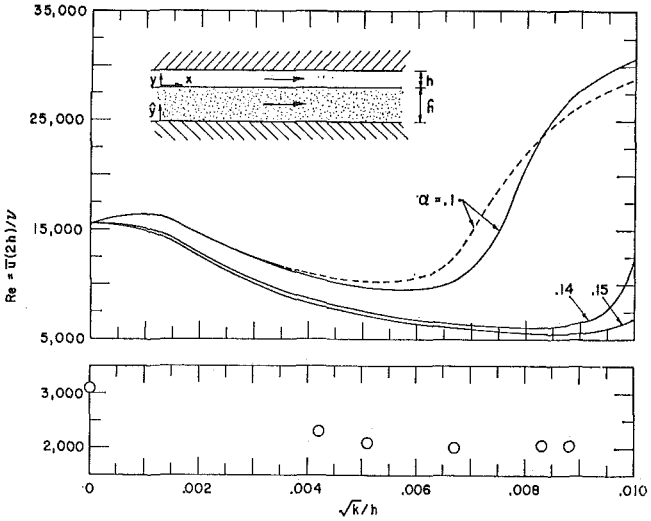

Fig. 1 Reynolds numbers marking laminar breakdown; upper graph, linear stability theory; lower graph, experiments

Formulation of the Stability Problem

A schematic diagram illustrating the problem under consideration is shown in Fig. 1. The lower bounding wall of the channel is permeable, while the upper is solid. The height of the channel and the thickness of the permeable material are, respectively, h and $\hat{h}$, and the corresponding transverse coordinates are y and $\hat{y}$. The axial coordinate is x. A circumflex is used to distinguish quantities that are specific to the permeable material from those for the channel.

The stability analysis begins with the flow in the channel. Superposed on the laminar main flow, it is assumed that there are small disturbances of the velocity components and of the static pressure. The disturbances are assumed to be of the plane wave type, and the stream function ψ' and static pressure p' characterizing the disturbance are expressed as

$$\psi'(x, y, t) = \phi(y) \exp [ia(x - ct)]$$
$$p'(x, y, t) = \pi(y) \exp [ia(x - ct)] \tag{1}$$

in which ϕ and π are amplitude functions, a is the wave number, and c is the wave velocity.

If it is assumed that the resultant flow (main flow plus disturbances) satisfies the Navier-Stokes equations and that quadratic disturbance terms are negligible, then the Orr-Sommerfeld equation for ϕ emerges

$$(U - c)(D^2 - a^2)\phi - \phi D^2 U = -(2i/a \text{ Re}) \times (D^4 - 2a^2D^2 + a^4)\phi. \tag{2}$$

In this equation, U is the main flow velocity distribution made dimensionless with respect to the mean velocity $\bar{u}$, and D is the differentiation operator d/dY, where $Y = y/h$. Also, a and c are now dimensionless with respect to the scales h and $\bar{u}$. The Reynolds number Re is based on the equivalent diameter which, for a parallel-plate channel, is $2h$, so that

$$\text{Re} = \bar{u}(2h)/\nu. \tag{3}$$

The main flow velocity distribution appearing in the Orr-Sommerfeld equation is skewed owing to velocity slip at the surface of the permeable wall [1, 2]. In a notation appropriate to the present analysis, the dimensionless velocity profile $U(Y)$ may be expressed as

$$U(Y) = \frac{6}{1 + 3f}(1 - Y)(Y + f) \tag{4}$$

in which

$$f(\sqrt{k}/h, \alpha) = \frac{(\sqrt{k}/\alpha h) + 2(\sqrt{k}/h)^2}{(\sqrt{k}/\alpha h) + 1}. \tag{5}$$

The quantities k and α are, respectively, the permeability of the porous material and the slip coefficient, both of which are found by experiment. The permeability is defined via Darcy's law, and the slip coefficient enters the problem through the slip boundary condition at the surface of the permeable wall. For the main flow, this condition has the form [1, 2]

$$\frac{du}{dy} = \frac{\alpha}{\sqrt{k}}(u - \hat{u}), \qquad y = 0 \quad \text{and} \quad \hat{y} = \hat{h} \tag{6}$$

in which u and $\hat{u}$ are, respectively, the velocities in the channel and in the permeable material; $\hat{u}$ is found from Darcy's law. It is worth noting that the basis of the slip boundary condition is the replacement of the boundary layer within the permeable material by a velocity discontinuity at the permeable surface.

Attention may next be turned to the permeable material. For an incompressible fluid (e.g., a liquid), the disturbance flow and pressure fields are governed by

$$\nabla \cdot \hat{\mathbf{u}}' = 0 \tag{7}$$

$$\frac{\rho}{\epsilon}\frac{\partial}{\partial t}(\hat{\mathbf{u}}') = -\nabla \hat{p}' - \frac{\mu}{k}\hat{\mathbf{u}}'. \tag{8}$$

The first of these is the equation of continuity, whereas the second is an unsteady form of Darcy's law [6]. The quantity ϵ is the porosity of the permeable material and ρ is the density of the fluid. The quadratic inertia terms have been omitted from equation (8) inasmuch as they are very small compared with the other terms appearing therein.

If the time-dependent portion of $\hat{\mathbf{u}}'$ and $\hat{p}'$ is embodied in exp $[ia(x - ct)]$, then equation (8) is equivalent to

Nomenclature

a = wave number
C_f = friction factor; $(-dp/dx)D_e/(\rho\bar{u}^2/2)$
c = wave velocity
D = differentiation operator, d/dY
D_e = equivalent diameter
h = height of channel
$\hat{h}$ = height of permeable material
k = permeability
p' = disturbance pressure in channel
$\hat{p}'$ = disturbance pressure in permeable material
Re = Reynolds number, $\bar{u}D_e/\nu$
t = time
U = dimensionless velocity, $u/\bar{u}$
u = main flow velocity distribution in channel
$\bar{u}$ = mean velocity
u_s = slip velocity
u', v' = disturbance velocity components in channel
$\hat{u}$ = main flow velocity distribution in permeable material
$\hat{\mathbf{u}}'$ = disturbance velocity vector in permeable material
$\hat{u}', \hat{v}'$ = disturbance velocity components in permeable material
x = axial coordinate
Y = dimensionless coordinate, y/h
$y, \hat{y}$ = transverse coordinates, Fig. 1
α = slip coefficient
ϵ = porosity
μ = viscosity
ν = kinematic viscosity
π = amplitude of disturbance pressure p'
ρ = density
ϕ = amplitude of disturbance stream function ψ'
ψ' = disturbance stream function

Superscript

* = solid-walled rectangular duct

$$\hat{u}' = -(k/\mu)\nabla\hat{p}' \Big/ \left(1 - \frac{i\rho ack}{\mu\epsilon}\right). \quad (9)$$

Equations (7) and (9) yield $\nabla^2\hat{p}' = 0$, a relevant solution of which is

$$\hat{p}' = (A \cosh a\hat{y} + B \sinh a\hat{y}) \exp [ia(x - ct)]. \quad (10)$$

One of the integration constants can be determined by noting that the transverse velocity $\hat{v}'$ is zero at the solid wall which bounds the permeable material from below. Upon evaluating $\hat{v}'$ from equations (9) and (10), one obtains

$$\hat{v}' = -\frac{(ka/\mu) \exp [ia(x - ct)](A \sinh a\hat{y} + B \cosh a\hat{y})}{1 - (i\rho ack/\mu\epsilon)}, \quad (11)$$

so that $B = 0$ to satisfy the aforementioned boundary condition.

Next, conditions of continuity are employed at the interface between the permeable material and the channel, $y = 0$ and $\hat{y} = \hat{h}$. These conditions facilitate the determination of the integration constant A that appears in equations (10) and (11) and, more importantly, provide a boundary condition for the Orr-Sommerfeld equation (2).

The transverse velocity and static pressure are required to be continuous at the interface. The transverse disturbance velocity v' in the channel is evaluated from the stream function ψ' in equation (1). After specializing the v' expression to $y = 0$, it is equated to $\hat{v}'$ at $\hat{y} = \hat{h}$ from equation (11). Since B is already zero, this gives

$$A = i\mu\phi(0)\left(1 - \frac{i\rho ack}{\mu\epsilon}\right) \Big/ k \sinh (a\hat{h}). \quad (12)$$

The continuity of the disturbance pressure field at the interface can be expressed via equations (1) and (10), with the result

$$\pi(0) = A \cosh (a\hat{h}). \quad (13)$$

In turn, the amplitude $\pi(0)$ is eliminated by employing the streamwise momentum equation for the disturbance flow in the channel. After incorporating the constant A from equation (12) and introducing dimensionless variables, one finds

$$\left\{\frac{2i}{a \text{ Re}}\left[D^3 - a^2D + \frac{a(h/\sqrt{k})^2}{\tanh (a\hat{h}/h)}\left(1 - \frac{iac(\sqrt{k}/h)^2 \text{ Re}}{2\epsilon}\right)\right]\phi + (U - c)D\phi - \phi DU\right\}_{Y=0} = 0. \quad (14)$$

Equation (14) serves as one of the boundary conditions for the Orr-Sommerfeld equation (2). It replaces the condition $\phi(0) = 0$ which would have been used to express the requirement that $v' = 0$ had the lower bounding wall of the channel been impermeable. Thus one of the important differences between the present stability analysis and that for a conventional channel flow is that the transverse disturbance velocity need not be zero at the bounding surface.

The other boundary conditions for the Orr-Sommerfeld equation will now be derived. At the permeable surface, the streamwise disturbance velocity obeys the slip boundary condition

$$\frac{du'}{dy} = \frac{\alpha}{\sqrt{k}}(u' - \hat{u}'), \quad (15)$$

in which $\hat{u}'$ is evaluated at $\hat{y} = \hat{h}$ and, with the aid of equations (9), (10), and (12), is expressible as

$$\hat{u}'(\hat{h}) = a\phi(0) \exp [ia(x - ct)]/\tanh (a\hat{h}). \quad (16)$$

Then, by employing the disturbance stream function in equation (1) to express u', the slip boundary condition takes the dimensionless form

$$(\sqrt{k}/a\hbar)D^2\phi = D\phi - \frac{a\phi}{\tanh (a\hat{h}/h)} \quad \text{at } Y = 0 \quad (17)$$

which replaces the condition $\phi'(0) = 0$ that would have applied had the wall been impermeable.

The upper bounding wall of the channel is impermeable, so that the usual condition of vanishing velocities is applicable. In conjunction with the first of equations (1), this gives

$$\phi = D\phi = 0 \quad \text{at } Y = 1. \quad (18)$$

The formulation of the stability problem for the channel flow is now complete. The disturbance amplitude ϕ is governed by the Orr-Sommerfeld equation (2), with the main flow velocity distribution being expressed by equation (4). The boundary conditions on ϕ and its derivatives are given by equations (14), (17), and (18). The mathematical system made up of the aforementioned equations is homogeneous, so that a, c, and Re participate in an eigenvalue problem. There are, in addition, four prescribable parameters which are specific to the present problem and are related to the presence of the permeable bounding wall. These parameters are $\sqrt{k}/h$, α, $\hat{h}/h$, and ϵ.

Before going on to the solutions and results, it may be of interest to point out certain similarities between the present stability problem and that for a boundary-layer flow. In the boundary-layer case, the disturbance velocities at the edge of the boundary layer are not required to be zero. Rather, they are constrained in such a way as to insure that the disturbances vanish asymptotically in free stream. Similarly, for the permeable-walled channel, zero disturbance conditions are not imposed at the permeable bounding surface. The disturbances diminish monotonically with increasing depth of penetration into the permeable material.

Solutions and Results

The eigenvalue problem that was formulated in the preceding section of the paper was solved numerically on an IBM 360/50 digital computer using double-precision complex arithmetic. The skewed main flow requires that the disturbance equation (2) be applied at all points in the channel cross section (rather than in half the cross section). Correspondingly, the region $0 \leq Y \leq 1$ was subdivided into 100 mesh points and the governing equations recast into finite-difference form by the method of Thomas [7]. The eigenvalues were determined from the condition that the determinant of the coefficients of the algebraic system be zero. In carrying out the numerical computations, the parameters $\sqrt{k}/h$, α, $\hat{h}/h$, and ϵ were assigned fixed values. Then, for a given pair of values for a and Re, c_r and $c_i (c = c_r + ic_i)$ were found so as to satisfy the zero determinant condition. Next, a (or Re) was varied so that $c_i = 0$ when the zero determinant condition was fulfilled. This gave a point on the neutral curve in the a, Re plane. The same procedure was repeated a number of times and a segment of the neutral curve mapped out. The critical Reynolds number corresponding to the assigned parameter values was then read from a large scale plot of the neutral curve.

Critical Reynolds numbers were determined for parametric values of $\sqrt{k}/h$ between 0 and 0.01, the choice of this range having been guided by the present experiments. The slip coefficient α was assigned values of 0.1, 0.14, and 0.15. The first of these α values was motivated by the results of [2], whereas the latter two values bracket the range of α encountered in the present experiments. The ratio $\hat{h}/h$ appears only in the term $\tanh (a\hat{h}/h)$. Since a is on the order of one and $\hat{h} > 10h$ for the experiments, the hyperbolic tangent was taken to be unity and $\hat{h}/h$ was not a parameter of the problem. Furthermore, since the porosities of the permeable materials used in the experiments were only slightly less than unity, ϵ was assigned a value of one for the stability computations.

Attention is now turned to the presentation and discussion of the critical Reynolds number results as shown in Fig. 1. In the figure, the critical Reynolds number is plotted as a function of $\sqrt{k}/h$ for parametric values of the slip coefficient α. Since the impermeable wall corresponds to $\sqrt{k}/h = 0$ and since the velocity slip increases with increasing $\sqrt{k}/h$ (as demonstrated in the discussion of the experimental results), this parameter can be regarded as a measure of the extent of the interaction between the channel flow and the permeable material. In addition to the three solid curves of the figure, respectively, for $\alpha = 0.1$, 0.14, and 0.15, there is also a dashed curve for $\alpha = 0.1$ whose significance will be discussed shortly. Discussion of the experimental points appearing in the lower part of the figure will be deferred until later in the paper.

As seen in Fig. 1, the curves of Re versus $\sqrt{k}/h$ have an undulating character, indicating a complex dependence of the linear stability limit on the various interactions between the channel and the permeable material. In certain ranges of $\sqrt{k}/h$, the critical Reynolds number is substantially reduced owing to the presence of the permeable bounding wall. The results may be made plausible by considering the several mechanisms by which the permeable material affects the linear stability limit of the channel flow. The nonvanishing of the transverse disturbance velocity at the permeable surface should be destabilizing. Also tending to destabilize the flow is the nonvanishing of the streamwise disturbance velocity at the permeable surface. On the other hand, the type of skewing of the main flow velocity profile which results from slip at the permeable bounding surface should provide increased stability (for instance, see [8], where the effect of velocity profile skewness was investigated).

It is also possible to identify the ranges of $\sqrt{k}/h$ where the various mechanisms predominate. In the range of $\sqrt{k}/h$ in which the curves show a decreasing tendency, the nonvanishing transverse disturbance velocity is believed to be the main factor. The influence of the slip coefficient α is relatively small within this range of $\sqrt{k}/h$, which is consistent with the fact that α does not appear in equation (14), which embodies the transverse velocity boundary condition. On the other hand, in the range of $\sqrt{k}/h$ in which the curves show an increasing tendency, the effect of skewness of the main flow velocity profile would appear to predominate. In this range, the role of α is quite pronounced, as might be expected from the main flow velocity distribution (4).

It is also interesting to observe that the destabilizing effect of the transverse velocity tends to persist to larger values of $\sqrt{k}/h$ at higher values of α. Furthermore, for both $\alpha = 0.14$ and 0.15, there is a range of $\sqrt{k}/h$ where the stabilizing and destabilizing factors tend to neutralize each other and Re is nearly independent of $\sqrt{k}/h$.

The dashed curve appearing in Fig. 1 represents results that correspond to a model in which a steady form of Darcy's law is used for the permeable material instead of the unsteady form. The use of the steady form causes the group $iac(\sqrt{k}/h)^2\,\mathrm{Re}/2\epsilon$ to be deleted from equation (14). From Fig. 1, it is seen that there is a modest quantitative influence of the form of Darcy's law on the stability results, while all of the qualitative trends are preserved. Additional computations showed that the critical Reynolds numbers were essentially unaffected by the retention or omission of the term $\hat{u}'$ in the slip boundary condition (15).

A listing of the critical Reynolds numbers and the corresponding dimensionless wave numbers a and wave speeds c_r is presented in Table 1.

Table 1 Critical Reynolds numbers and related results

α	$\sqrt{k}/h$	Re	a	c_r
0.1	0	15520	2.04	0.396
	1/2000	16160	2.02	0.391
	1/1000	16390	2.00	0.391
	1/600	15320	1.99	0.400
	1/400	13370	1.99	0.414
	1/250	10650	1.94	0.434
	1/200	9688	1.89	0.442
	1/150	10280	1.75	0.439
	1/135	14180	1.61	0.410
	1/125	20940	1.50	0.375
	1/100	30720	1.40	0.338
0.14	0	15520	2.04	0.396
	1/1000	15120	2.03	0.398
	1/400	11500	2.07	0.426
	1/200	7480	2.09	0.471
	1/150	6320	2.05	0.488
	1/125	6056	1.98	0.493
	1/110	6696	1.86	0.482
	1/104	8512	1.73	0.458
	1/100	12540	1.60	0.421
0.15	0	15520	2.04	0.396
	1/1000	14940	2.03	0.398
	1/400	11220	2.09	0.428
	1/200	7172	2.13	0.475
	1/150	5944	2.10	0.496
	1/125	5504	2.05	0.504
	1/110	5604	1.97	0.502
	1/100	6888	1.81	0.480

Experiments

Apparatus. Experiments were undertaken to investigate the relationship between the Reynolds number marking the breakdown of the laminar regime and the magnitude of the slip velocity. The experiments were performed utilizing a closed-loop fluid-flow facility which, except for minor modifications, was the same as that of [2]. The test section was designed so that flat rectangular ducts of various heights could be obtained. The lower wall of each duct was a block of permeable material (FOAMETAL) which has the property that there are no free fiber ends within the material. The upper wall and the side walls were of impermeable materials. The cross-sectional aspect ratios (width/height) of all the ducts used in the experiments exceeded 55.

The working fluid, demineralized water, passed into the test section from an upstream plenum chamber and flowed in parallel paths through the rectangular duct and the permeable material. The inlet configuration was square-edged. At the downstream end of the test section, the effluxes from the duct and the permeable material were directed into separate plenum chambers. The liquid levels in the upstream plenum chamber and in each of the downstream plenum chambers could be independently set. In this way, transverse pressure differences could be eliminated and identical axial pressure gradients obtained for the flows in the duct and in the permeable material.

Measurements were made of the static pressure distributions along the upper bounding wall of the duct and along the lower bounding wall of the permeable material. The rates of mass flow through the duct and the permeable material were also measured. The permeability k of the porous material was measured at two different times during the course of the research, yielding the mean value $k = 4.5 \times 10^{-7}$ cm^2, with a scatter of ± 3 percent.

A set of flow visualization experiments was also performed. For these, a neutrally buoyant dye filament was introduced through a hypodermic tube situated at the inlet cross section of the duct and observations were made through a plexiglass plate which served as the upper bounding wall of the duct.

Some experiments were carried out in which the permeable bounding wall was replaced by an impermeable wall, so that all

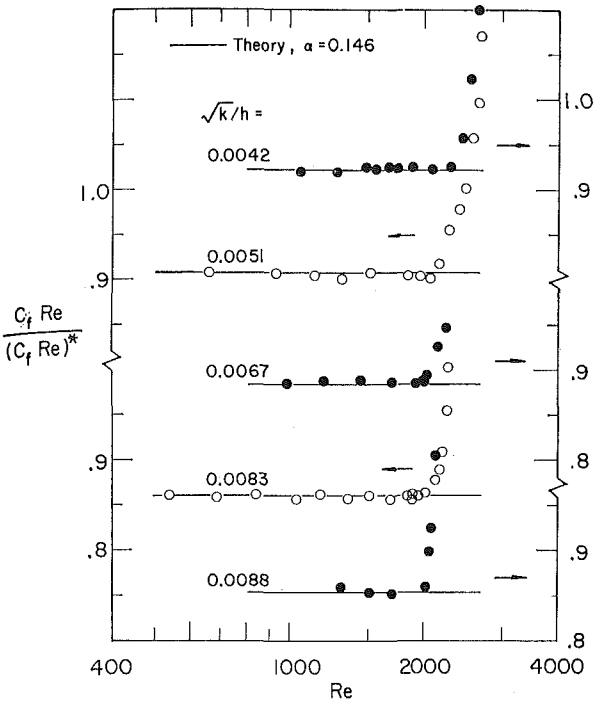

Fig. 2 Friction coefficient results indicating breakdown of laminar flow

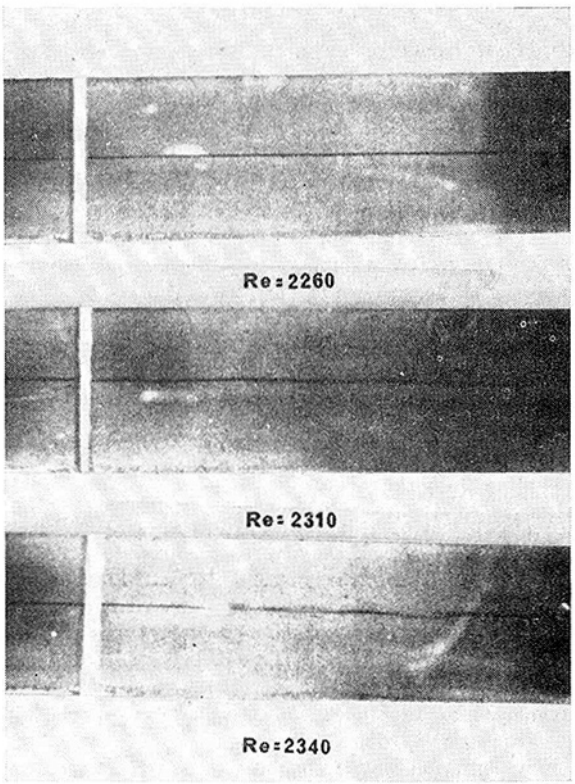

Fig. 3 Flow visualization evidence of the breakdown of laminar flow; $\sqrt{k}/h = 0.0042$

duct boundaries were impermeable. The square-edged inlet geometry remained as before.

Results and Discussion. Equations (4) and (5), when evaluated at $y = 0$, indicate that the slip velocity ratio $u_s/\bar{u}$ depends on $\sqrt{k}/h$ and α. For a given permeable material (fixed values of k and α), as in the present experiments, $u_s/\bar{u}$ varies with the channel height h, increasing as h decreases. Thus $\sqrt{k}/h$ serves as an appropriate dimensionless grouping to characterize the magnitude of the slip velocity, with $u_s/\bar{u}$ increasing with increasing values of $\sqrt{k}/h$.

For a fixed slip velocity ratio characterized by a fixed value of $\sqrt{k}/h$, we shall use the behavior of the friction factor—Reynolds number product to identify the breakdown of the laminar regime. The C_f Re product is independent of the Reynolds number in the laminar regime but varies with the Reynolds number in the transition and turbulent regimes. Fig. 2 shows the experimental values of C_f Re plotted as a function of the Reynolds number for parametric values of $\sqrt{k}/h$. To provide further insights, to be discussed shortly, we have used C_f Re/$(C_f$ Re$)^*$ as the ordinate variable, where $(C_f$ Re$)^*$ corresponds to a solid-walled rectangular duct. Both C_f Re and $(C_f$ Re$)^*$ correspond to the same aspect ratio AR. For large values of AR, $(C_f$ Re$)^*$ is given by [9]

$$(C_f \text{ Re})^* = \frac{96}{1 - (192/\pi^5 AR)} \left(\frac{AR}{AR + 1}\right)^2. \qquad (19)$$

Reynolds numbers characterizing laminar breakdown were identified by careful examination of Fig. 2 and are plotted in the lower graph of Fig. 1 as a function of $\sqrt{k}/h$. Also appearing there is the breakdown Reynolds number for the impermeable-walled duct ($\sqrt{k}/h = 0$) as reported in [2] and corroborated during the course of the present investigation. From an inspection of the graph, it is seen that the breakdown Reynolds number is significantly lower in the presence of velocity slip than for a solid-walled duct having the same entrance configuration and comparable aspect ratio. For the permeable-walled ducts ($\sqrt{k}/h > 0$), it appears that the breakdown Reynolds number first decreases with increasing slip velocity and then tends to remain relatively constant.

The just-presented results for the breakdown Reynolds number are supported by the findings of the flow visualization experiments. Photographic information from these experiments is shown in Fig. 3 for the case characterized by $\sqrt{k}/h = 0.0042$. The figure contains three photos corresponding, respectively from top to bottom, to Re = 2260, 2310, and 2340. When Re = 2260, the dye filament is straight and steady, thereby indicating laminar flow. Slight irregularities in the filament are in evidence in the photograph for Re = 2310, showing that the flow is no longer strictly laminar. When Re = 2340, the filament is subjected to somewhat greater disturbances. The photographs suggest a breakdown Reynolds number slightly less than 2310, which is in excellent accord with the value of 2300 inferred from the friction coefficient experiments. Since the flow visualization experiments were performed without pressure taps in the duct walls, the just-mentioned good agreement indicates that the pressure tap openings did not create disturbances which affected laminar breakdown.

Attention is now redirected to Fig. 2 with a view to discussing other aspects of the results presented there. In view of the fact that C_f Re/$(C_f$ Re$)^* = 1$ for a solid-walled duct, and noting that this ratio is less than one for all cases in Fig. 2, it is evident that velocity slip acts to decrease the friction coefficient. The extent of the decrease is accentuated with increasing values of $\sqrt{k}/h$, that is, as the $u_s/\bar{u}$ ratio increases.

The laminar data presented in Fig. 2 can also be employed to evaluate the so-called slip coefficient α for the permeable material of the experiments. The coefficient α was introduced in [1] in connection with a model used therein to characterize the slip velocity. Application of that model to fully developed laminar flow in a parallel-plate channel having one permeable bounding wall yields

$$\frac{C_f \text{ Re}}{(C_f \text{ Re})^*} = \left[1 + \frac{3(\sigma + 2\alpha)}{\sigma(1 + \alpha\sigma)}\right]^{-1}, \qquad \sigma = h/\sqrt{k}. \qquad (20)$$

The quantity C_f Re/$(C_f$ Re$)^*$ is essentially independent of aspect

ratio for rectangular ducts of sufficiently large aspect ratio, although both C_f Re and $(C_f \text{ Re})^*$ may vary with aspect ratio [10].

With C_f Re from experiment, $(C_f \text{ Re})^*$ from equation (19), and the known values of $\sqrt{k}/h$, equation (20) was employed to evaluate α for 50 experimental runs in the laminar regime. The resulting values ranged between 0.14 and 0.15, with a mean value of 0.146. The variation of α within the just-mentioned range is largely due to the slight scatter of the experimental data. With this in mind, it may be concluded that α is essentially a constant for the 50 different experimental conditions employed. This constancy of α is supportive of the velocity slip model. The horizontal lines shown in Fig. 2 represent the predictions of equation (20) corresponding to the mean value of 0.146 for α.

From equation (4) with $y = 0$, it can be calculated that the slip velocity ratio $u_s/\bar{u}$ varies from 0.15 to 0.3 over the range of $\sqrt{k}/h$ from 0.0042 to 0.0088, which characterized the experiments.

Concluding Remarks

We now return to Fig. 1 to discuss briefly the relationship between the analytical and the experimental results. Since the α values of the experiments lie between 0.14 and 0.15, the analytical curves for these α are relevant to the present discussion. In the range of $\sqrt{k}/h$ of the permeable-wall experiments, both the analytical and experimental results fall below the corresponding values for the impermeable wall. Furthermore, in this range, both analysis and experiment indicate that the Reynolds number is relatively insensitive to $\sqrt{k}/h$.

For impermeable-walled channels, it is well known that the instability Reynolds number given by linear theory is substantially higher than the experimentally determined breakdown Reynolds number (for example, Fig. 1 at $\sqrt{k}/h = 0$). This same situation continues to prevail for permeable-walled ducts. It should be noted, however, that the ratio of the critical Reynolds number from theory to the corresponding breakdown Reynolds number from experiment decreases by a factor of two as $\sqrt{k}/h$ increases from zero to 0.0088.

Acknowledgments

The authors wish to thank Prof. D. D. Joseph for the formulation of the analysis concerning the coupling of the disturbance fields. The support of the National Science Foundation under Grants GK 13303 and GK 4839 is gratefully acknowledged.

References

1 Beavers, G. S., and Joseph, D. D., "Boundary Conditions at a Naturally Permeable Wall," *Journal of Fluid Mechanics*, Vol. 30, 1967, pp. 197–207.

2 Beavers, G. S., Sparrow, E. M., and Magnuson, R. A., "Experiments on Coupled Parallel Flows in a Channel and a Boundin Porous Medium," *Journal of Basic Engineering*, TRANS. ASME, Vol. 92, Series D, 1970, pp. 843–848.

3 Saffman, P. G., "On the Boundary Condition at the Surface of a Porous Medium," *Studies in Applied Mathematics*, Vol. 50, 1971, pp. 93–101.

4 Taylor, G. I., "A Model for the Boundary Condition of a Porous Material. Part 1," *Journal of Fluid Mechanics*, Vol. 49, 1971, pp. 319–326.

5 Richardson, S., "A Model for the Boundary Condition of a Porous Material. Part 2," *Journal of Fluid Mechanics*, Vol. 49, 1971, pp. 327–336.

6 Wankat, P. C., and Schowalter, W. R., "Stability of Combined Heat and Mass Transfer in a Porous Medium," *Physics of Fluids*, Vol. 13, 1970, pp. 2418–2420.

7 Thomas, L. H., "The Stability of Plane Poiseuille Flow," *Physical Review*, Vol. 91, 1953, pp. 780–783.

8 Fu, T. S., and Joseph, D. D., "Linear Instability of Asymmetric Flow in Channels," *Physics of Fluids*, Vol. 13, 1970, pp. 217–221.

9 Lundgren, T. S., Sparrow, E. M., and Starr, J. B., "Pressure Drop Due to the Entrance Region in Ducts of Arbitrary Cross Section," *Journal of Basic Engineering*, TRANS. ASME, Vol. 86, Series D, 1964, pp. 620–626.

10 Masha, B. A., Private Communication, 1971.